Acta Physiologiae Plantarum (2018) 40:31
https://doi.org/10.1007/s11738-018-2613-z

SHORT COMMUNICATION

How the surface properties affect the nanocytotoxicity of silver? Study of the influence of three types of nanosilver on two wheat varieties

Barbasz Anna[1] · **Kreczmer Barbara**[1] · **Oćwieja Magdalena**[2]

Received: 21 June 2017 / Revised: 9 January 2018 / Accepted: 10 January 2018 / Published online: 17 January 2018

Abstract
The influence of silver nanoparticles on calli cells of stress tolerant—Parabola and stress sensitive—Raweta wheat genotypes (*Triticum aestivum* L.) was studied. Three types of silver nanoparticles (AgNPs) were tested: cystamine-stabilized (positively charged), unmodified, synthesized using sodium borohydride and citrate-stabilized AgNPs, both negatively charged. Physico-chemical properties of silver nanoparticles were investigated by: UV–Vis spectroscopy, dynamic light scattering used for electrophoretic mobility and hydrodynamic diameter determination and transmission electron microscopy. The evaluation of cytotoxicity was estimated basing on lipid peroxidation, proline content and antioxidant enzymes activity. For sensitive variety every type of nanoparticles induced stress (proline increase) in cells, but positively charged nanoparticles were most cytotoxic. Treatment of stress tolerant Parabola by AgNPs caused the increase in SOD activity, suggesting the occurrence of oxidative stress in cells, confirmed by the increase of membrane lipid peroxidation. Negatively charged AgNPs were significantly more cytotoxic to the calli cells of sensitive variety in comparison to tolerant one.

Keywords Wheat · Callus · Silver nanoparticles · Cytotoxicity

Introduction

Cytotoxicity and genotoxicity of metallic nanoparticles have been confirmed for many types of animal cells, being associated with various methods of synthesis, particles` shapes, sizes, etc. Exact mechanism of metallic nanoparticles toxicity has not been yet elucidated. Today, the most widespread are silver nanoparticles (AgNPs). They are applied in many areas of life, medicine and technology. AgNPs exhibit biostatic properties against bacteria, fungi and viruses (Marambio-Jones and Hoek 2010). It is considered whether their cytotoxicity is related to particles themselves or to silver ions released from their surface. Plant cells are confined within a cell wall which is absent in animal cells, that undoubtedly constitutes an additional barrier. The pores in the wall of plant root cells usually have a diameter of 3–8 nm that is significantly smaller than most of the AgNPs analyzed (Carpita and Gibeaut 1993). Studies of AgNPs impact on bacteria have shown that in the presence of AgNPs, new pores in cell wall are formed which in consequence affects transmembrane transport (Pal et al. 2007). Several studies have shown that metal nanoparticles may influence plant physiology including seed germination, growth and cellular metabolism (Barbasz et al. 2016). AgNPs led to a reduction of mitochondrial function, cell membrane damage and oxidative stress causing cell injury (Barbasz et al. 2015; Gorczyca et al. 2015). The presence of AgNPs promotes oxidative stress generating reactive oxygen species (ROS).

In current work, we aimed at studying the influence of three types of AgNPs being similar in size distribution but differing in their surface properties. The surface properties of AgNPs, such as charge and oxidation state, depend on the physico-chemical characteristics of stabilizing agent (Kujda et al. 2015; Silva et al. 2014). It has been shown that positively charged AgNPs which are more prone to oxidative dissolution independently of their size exhibit higher toxicity for living organisms (Kittler et al. 2010; Silva et al. 2014). AgNPs are frequently used as a component of plant

Communicated by G. Klobus.

✉ Barbasz Anna
anna.barbasz@op.pl

[1] Institute of Biology, Pedagogical University, Podchorążych 2, 30-084 Kraców, Poland

[2] Jerzy Haber Institute of Catalysis and Surface Chemistry, Polish Academy of Sciences, Niezapominajek 8, 30-239 Kraców, Poland

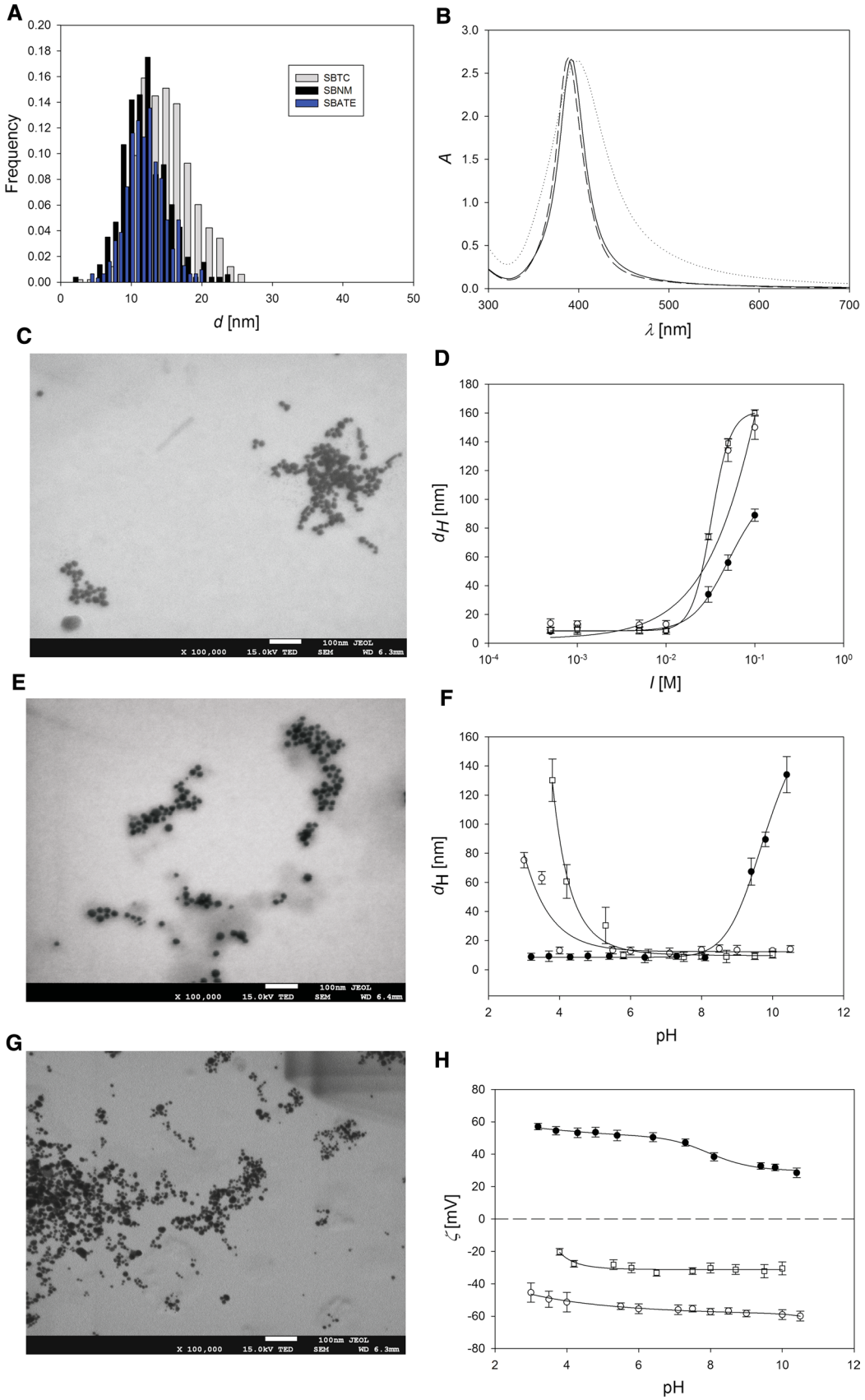
A
Frequency
d [nm]
SBTC
SBNM
SBATE
B
A
λ [nm]
C
X 100,000 15.0kV TED SEM WD 6.3mm
100nm JEOL
D
dH [nm]
I [M]
E
X 100,000 15.0kV TED SEM WD 6.4mm
100nm JEOL
F
dH [nm]
pH
G
X 100,000 15.0kV TED SEM WD 6.3mm
100nm JEOL
H
ζ [mV]
pH

◂**Fig. 1** Characteristics of AgNPs. **a** Size distribution of nanoparticles obtained basing on TEM analyses; **b** the UV–Vis spectra of silver suspensions: straight line, SBNM; broken line, SBTC; dotted line, SBATE recorded for a bulk concentration of 20-25 mg dm^{-3}; typical TEM micrographs of AgNPs; **c** SBNM, **e** SBTC, **g** SBATE and; **d** hydrodynamic diameter of AgNPs: open squares, SBNM; open circles, SBTC and filled circles, SBATE as a function of ionic strength at pH 5.5 and **f** hydrodynamic diameter of AgNPs as a function of pH for ionic strength equal to 0.01 mol dm^{-3}. The measurements were carried out by DLS technique for the silver suspension concentration of 30 mg dm^{-3} and temperature of 298 K. **h** Dependence of the zeta potential of AgNPs: open squares, SBNM, open circles, SBTC and filled circles, SBATE on ionic strength at pH 5.5 and $T = 298$ K. The solid lines in **d**, **f** and **h** represent nonlinear fit to experimental data

protection products, although it is not completely clear how AgNPs interact with plant cells. In previous work we have shown that oxidative stress in wheat cells generated by AgNPs results from the osmotic stress, and both particles and silver ions may cause similar cytotoxicological results (Barbasz et al. 2016). Current studies are focused on determination of cytotoxic effects of three types of AgNPs (cystamine-stabilized, positively charged) (SBATE), unmodified, obtained using sodium borohydride (SBNM) and citrate-stabilized AgNPs (SBTC), both negatively charged on callus cells of two varieties of spring wheat (*Triticum aestivum* L.) Parabola and Raweta.

Materials and methods

Synthesis and characteristics of silver nanoparticle suspensions

Silver suspensions were prepared by chemical reduction of silver salt.

SBTC suspension

1 mmol dm^{-3} silver nitrate solution was added to the reduction mixture containing 64 mg sodium borohydride and 560 mg trisodium citrate 200 cm^3. The whole was shaken for one hour at the room temperature.

SBNM suspension

160 cm^3 of 2.5 mmol dm^{-3} silver nitrate solution was added to sodium borohydride solution (2.5 cm^3, 10 mmol dm^{-3}) and mixed at room temperature for 30 min.

SBATE suspension

After preparing the mixture as in the recipe above and 5-min mixing, 5 cm^3 of 1.42 mmol dm^{-3} aqueous solution of cysteamine hydrochloride was added. The mixing was continued for 1 h.

The physico-chemical properties of AgNPs were monitored by UV–Vis measurements. Nanoparticles` diffusion coefficients at various pH and temperatures were measured by dynamic light scattering (DLS) with Zeta-Sizer Nano ZS apparatus. The same instrument was used to determine the electrokinetic properties of nanoparticles. Knowing nanoparticles` electrophoretic mobility and hydrodynamic diameter, the values of zeta potential were calculated using Henry's equation (Oćwieja et al. 2011). The size distribution and morphology of silver nanoparticles were determined by transmission electron microscopy (TEM).

Cell culture

Wheat (*T. aestivum* L.) calli were produced from immature embryos. Wheat embryos were sterilized in 70% ethanol for 1 min, then in 10% solution of bleaching agent ("Domestos") for 10 min. The embryos were rinsed in sterile water and placed on Petri dishes containing Murashige and Skoog (MS) medium supplemented with 2,4-D (2 mg dm^{-3}) to receive undifferentiated calli (procedure from Filek et al. 2009). After 3 months of culture, randomly selected (from several scabs) 1 g of calli tissue was transferred into 20 cm^{-3} MS medium containing AgNPs in subsequent concentrations. Each AgNPs concentration was applied three times (three technical replicates). After 24 h the biochemical analysis were made.

Determination of lipid peroxidation

About 1 g of calli was homogenized with 5 cm^3 of 0.5% trichloroacetic acid (TCA) and after centrifugation at 1000×*g*, 1 cm^3 of the supernatant was mixed with 4 cm^3 of 0.5% thiobarbituric acid (TBA) in 20% TCA. The mixture was boiled for 30 min and concentration of malondialdehyde (MDA) (lipid peroxidation indicator) was determined spectrophotometrically at 532 nm. The molar extinction coefficient of MDA was taken to be equal to 155×10^5 $mmol^{-1}$ cm^{-1}.

Proline concentration

1 g of calli was homogenized in 3 cm^3 of 3% aqueous sulfosalicylic acid and centrifuged at 1000×*g*. 0.5 cm^3 of supernatant was added to 1 cm^3 of 1% ninhydrin in 60% acetic acid and the samples were incubated for 20 min at 100 °C. After cooling, the reaction mixture was extracted with 3 cm^3 toluene. The absorbance was measured at $\lambda = 525$ nm. The proline content was calculated from the calibration curve.

Enzyme assays

Approximately, 1 g of calli was homogenized in 0.05 mol dm^{-3} phosphate buffer (pH 7.2) containing 0.1 mmol dm^{-3} EDTA and 0.1% bovine serum albumin. The homogenate was centrifuged for 10 min at 10,000×*g*. Total superoxide dismutases activity [SOD; EC 1.15.11] was assayed according to spectrophotometric cytochrome method. Xanthine oxidase and supernatant were added to the reaction mixture consisting of phosphate buffer (pH 7.2), 0.1 mmol dm^{-3} EDTA, 0.1 mmol dm^{-3} cytochrome C, 0.1 mmol dm^{-3} xanthine. Measurements of absorbance at $\lambda = 550$ nm was performed for 2 min. It is assumed that the unit of activity (1 unit, 1 unit of cytochrome) corresponds to that amount of enzyme which causes 50% inhibition of cytochrome C reduction at 25 °C.

Statistical analysis

All biochemical analyses were repeated three times and averaged (± SD). The statistical significances of the means were assessed using the SAS ANOVA procedure. The results were analyzed by Duncan's multiple range test and *t* test at $p < 0.05$ using PC SAS 8.0. The statistical tests were run using STATISTICA 10.0 software.

Results and discussion

The obtained colloidal systems were characterized using various physicochemical techniques. The extinction spectra of diluted suspensions were recorded to confirm whether the optical properties are related to surface plasmon excitation of nanoparticles. As can be seen in Fig. 1b, each of the obtained suspensions exhibits a single characteristic absorption band near the 400 nm indicating that nanoparticles have spherical shape. The absorption maximum of SBATE suspension appears at a wavelength of 404 nm whereas the maxima of other suspensions are in the range of 389–391 nm. Recorded peaks are rather narrow, symmetric and do not have a shoulder in the region of higher wavelengths, what suggests that the suspensions are fairly monodisperse. Pictures taken from transmission electron microscope were used for determination of nanoparticles morphology and size distribution. The typical TEM micrographs of nanoparticles are presented in Fig. 1c, e, g. One can notice that nanoparticles are approximately spherical and exhibit similar size distribution (Fig. 1a). The average sizes of nanoparticles, obtained from histograms vary within a range of 11–14 nm. The diffusion coefficients of AgNPs in the suspensions of known pH and conductivity were determined by dynamic light scattering technique (DLS). Knowing the values of diffusion coefficients and using the Stock–Einstein relationship, the hydrodynamic diameters of nanoparticles were calculated. Then, the stock suspensions were diluted to particle concentration equal to 30 mg dm^{-3}. The changes in particle diffusion coefficients with ionic strength regulated by sodium chloride were monitored. The results of these experiments are presented in Fig. 1d as the dependence of nanoparticles` hydrodynamic diameter on ionic strength. Significant increase in ionic strength causes aggregation of silver nanoparticles which is manifested as changes of their hydrodynamic diameter. For ionic strength below 10^{-2} mol dm^{-3}, the average values of nanoparticle hydrodynamic diameters remain constant. This allows to conclude that irrespective of the method of preparation, silver nanoparticle suspensions are stable in similar range of ionic strengths.

Stability of the suspensions stabilized during the synthesis with agents of various chemical structure was determined under constant value of ionic strength equal to 10^{-2} mol dm^{-3} NaCl and varying pH regulated by the addition of sodium hydroxide or hydrochloric acid. The hydrodynamic diameter of nanoparticles as a function of pH was presented in Fig. 1f. These dependencies show that in the pH range between 5.5 and 8.1, the hydrodynamic diameter of each type of nanoparticles assumes a constant value. For the same experimental conditions, the electrophoretic mobility of the silver nanoparticles was measured and used for zeta potential calculations (Fig. 1h). As indicated by the negative values of nanoparticle zeta potential SBNM and the SBTC nanoparticles are negatively charged within an entire range of ionic strength. SBATE nanoparticles exhibit positive values of the zeta potential which suggests that they are positively charged. For all studied nanoparticles, an increase of ionic strength results in a decrease of absolute values of zeta potential what is related to a compression of electric double layer.

The fully characterized three types of nanoparticles were used for testing the plant cells. To check how the three types of tested AgNPs affect the cell membranes, the MDA content was determined. The degree of peroxidation of membrane lipids is generally expressed by the level of MDA. Treatment of cells with AgNPs caused an increase in MDA concentration in both tested varieties. A greater change (about 50%) was noticed for sensitive Raweta variety in comparison to Parabola treated by negatively charged AgNPs. But the level of MDA after treatment with SBATE (+) nanoparticles was greater for Parabola callus cells (at 5 mg dm^{-3} AgNPs). It is worth noting that in case of Parabola, the highest increase in membrane lipid peroxidation was observed after application of positively charged SBATE (at 5 mg dm^{-3}) (100% in comparison to control). For the sensitive Raweta the MDA level increases after treatment with all three types of AgNPs (less than 50% in comparison to control).

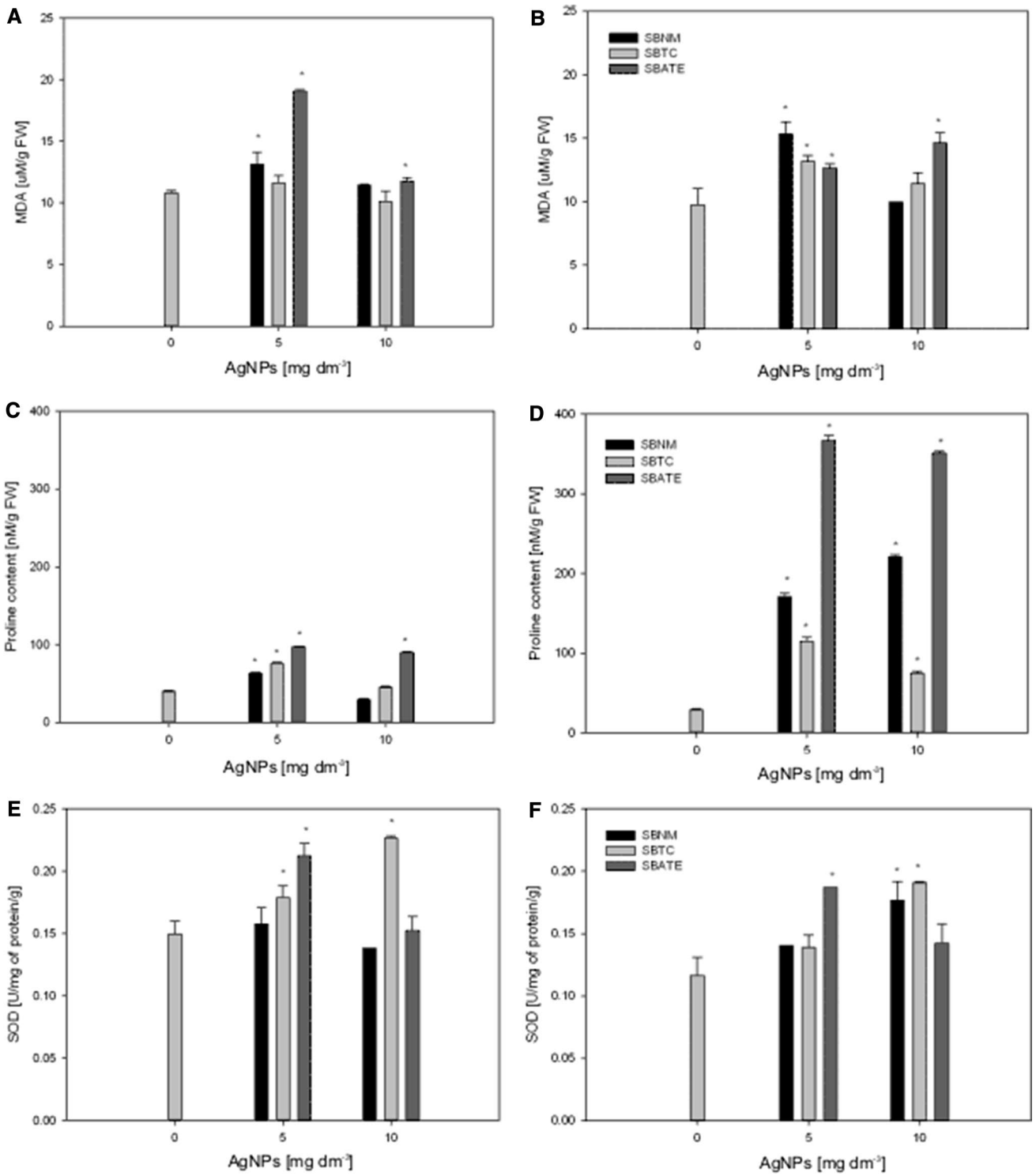

Fig. 2 Comparison of malondialdehyde (MDA) level in callus cells of Parabola (**a**) and Raweta (**b**) cultured on control media (0) and after 24 h exposure to AgNPs. Proline concentrations in callus cells of Parabola (**c**) and Raweta (**d**) after culture on control media (0) and after 24-h treatment by three types of AgNPs. Superoxide dismutase (SOD) activity in callus cells of Parabola (**e**) and Raweta (**f**) after culture on control media (0) and after 24 h exposure to AgNPs. Values represent the mean ± SD. Significant difference compared to controls ($p < 0.05$) was marked by stars

The concentration of osmoprotectant, proline was also analyzed. Proline is an excellent index of the stress experienced by plants. Jiang et al. (2012) investigated the *Spirodela polyrhiza* and noticed an increased concentration of proline after its treatment by AgNPs. The content of proline was significantly higher in Raweta than in Parabola cells. For both varieties, the most stressogenic were SBATE nanoparticles. However, the biggest changes versus control were reported after treatment of Raweta callus cells with SBATE at concentrations of 5 and 10 mg dm^{-3} (approximately ninefold increase of proline concentration) (Fig. 2d). In this case, the role of surface charge seems to be most important. Treatment of susceptible variety (Raweta) with AgNPs results in more than threefold increase of proline level compared to the resistant variety (Parabola).

Changes in activity of SOD in calli cells caused by contact with AgNPs indicate oxidative stress and ROS action in cells (Fig. 2e, f). SOD activity was significantly higher in comparison to the control and was dependent on dose and type of nanoparticles. For both wheat cultivars at AgNPs concentration equal to 5 mg dm^{-3}, the highest SOD activity was induced by SBATE, while at 10 mg dm^{-3}—by SBTC (both about 25% of the control). The results obtained clearly indicate the highest cytotoxicity of SBTC. Treatment of calli of both wheat cultivars by SBNM did not significantly influence SOD activity. Positively charged AgNPs have been shown to be the most toxic to bacteria and animal cells (Kujda et al. 2015; Silva et al. 2014). Also our research shows that AgNPs with positive charge (SBATE) are the most toxic to the cells tested. In the present study, biochemical parameters (MDA, proline, SOD) were used to determine whether AgNPs can induce oxidative stress in the calli cells of two wheat varieties. The significant increase of SOD activity indicates that exposure of cells to AgNPs initiates these enzymes action that helps ROS scavenging. Increased activity of antioxidant enzymes after exposure of cells to AgNPs was also demonstrated, among others in Oukarroum et al. (2013) and Jiang et al. (2014).

AgNPs act on the calli cells in many ways. The mechanism of AgNPs cytotoxicity is a combination of the effects of surface charge and a release of silver ions from nanoparticles. It can be stated that the surface charge of AgNPs is crucial for the development of responses of calli cells to stress action. In conclusion it can be stated that in the susceptible variety (Raweta) stress caused by AgNPs is significantly higher than in the resistant variety (Parabola). Each type of nanoparticles induces stress (which is well illustrated by the increase in proline concentration), but positively charged nanoparticles (SBATE) are most cytotoxic to the test cells. In the resistant variety (Parabola) the main effect of the presence of AgNPs was an increase in SOD, suggesting the occurrence of oxidative stress in the cells. For this variety, SBATE also proved to be the most cytotoxic. The present study was conducted on callus cells, which are undifferentiated plant cells. These cells are more sensitive to any xenobiotic. Their answer may differ from the response of the whole plant. In the further stages of research, we plan to perform infiltration of AgNPs into whole wheat plants and to introduce AgNPs of modified surface properties.

Author contribution statement AB and BK designed the research; AB, BK and MO conducted the research and analyzed the data. AB and BK wrote the paper; AB had primary responsibility for the final content. All authors have read and approved the final manuscript.

Acknowledgements This work was financially supported by Polish Ministry of Science and Higher Education (MNiSW) under Iuventus Plus No. IP 2015 055974 Grant.

References

Barbasz A, Oćwieja M, Barbasz J (2015) Cytotoxic activity of highly purified silver nanoparticles sol against cells of human immune system. Appl Biochem Biotechnol 176(3):817–834

Barbasz A, Kreczmer B, Oćwieja M (2016) Effects of exposure of callus cells of two wheat varieties to silver nanoparticles and silver salt ($AgNO_3$). Acta Physiol Plant 38(3):1–11

Carpita NC, Gibeaut DM (1993) Structural models of primary cell walls in flowering plants: consistency of molecular structure with the physical properties of the walls during growth. Plant J 3(1):1–30

Filek M, Zembala M, Hartikainen H, Miszalski Z, Kornaś A, Wietecka-Posłuszny R, Walas P (2009) Changes in wheat plastid membrane properties induced by cadmium and selenium in presence/absence of 2,4-dichlorophenoxyacetic acid. Plant Cell Tissue Organ Cult 96(1):19–28

Gorczyca A, Pociecha E, Kasprowicz M, Niemiec M (2015) Effect of nanosilver in wheat seedlings and *Fusarium culmorum* culture systems. Eur J Plant Pathol 142(2):251–261

Jiang HS, Li M, Chang FY, Li W, Yin LY (2012) Physiological analysis of silver nanoparticles and AgNO3 toxicity to *Spirodela polyrhiza*. Environ Toxicol Chem 31(8):1880–1886

Jiang HS, Qiu XN, Li GB, Li W, Yin LY (2014) Silver nanoparticles induced accumulation of reactive oxygen species and alteration of antioxidant systems in the aquatic plant *Spirodela polyrhiza*. Environ Toxicol Chem 33(6):1398–1405

Kittler S, Greulich C, Diendorf J, Koller M, Epple M (2010) Toxicity of silver nanoparticles increases during storage because of slow dissolution under release of silver ions. Chem Mater 22(16):4548–4554

Kujda M, Oćwieja M, Adamczyk Z, Bocheńska O, Braś G, Kozik A, Barbasz J (2015) Charge stabilized silver nanoparticles applied as antibacterial agents. J Nanosci Nanotechnol 15(5):3574–3583

Marambio-Jones C, Hoek EM (2010) A review of the antibacterial effects of silver nanomaterials and potential implications for human health and the environment. J Nanopart Res 12(5):1531–1551

Oćwieja M, Adamczyk Z, Morga M, Michna A (2011) High density silver nanoparticle monolayers produced by colloid self-assembly on polyelectrolyte supporting layers. J Colloid Interface Sci 364:39–48

Oukarroum A, Barhoumi L, Pirastru L, Dewez D (2013) Silver nanoparticle toxicity effect on growth and cellular viability of the aquatic plant *Lemna gibba*. Environ Toxicol Chem 32(4):902–907

Pal S, Tak YK, Song JM (2007) Does the antibacterial activity of silver nanoparticles depend on the shape of the nanoparticle? A study of the gram-negative bacterium *Escherichia coli*. Appl Environ Microbiol 73(6):1712–1720

Silva T, Pokhrel LR, Dubey B, Tolaymat TM, Maier KJ, Liu X (2014) Particle size, surface charge and concentration dependent ecotoxicity of three organo-coated silver nanoparticles: comparison between general linear model-predicted and observed toxicity. Sci Total Environ 468:968–976